Optical Modulation of Effective On-Site Coulomb Energy for the Mott Transition in an Organic Dimer Insulator

Y. Kawakami,[1] S. Iwai,[1,2,*] T. Fukatsu,[1] M. Miura,[1] N. Yoneyama,[2,3] T. Sasaki,[2,3] and N. Kobayashi[3]

[1]*Department of Physics, Tohoku University, Sendai 980-8578, Japan*

[2]*JST, CREST, Sendai 980-8578, Japan*

[3]*Institute for Materials Research, Tohoku University, Sendai 980-8577, Japan*

(Received 26 June 2009; published 7 August 2009)

We report an optical modulation of the effective on-site Coulomb energy U on a dimer (U_{dimer}) for achieving the Mott insulator-to-metal transition in κ-(BEDT-TTF)$_2$Cu[N(CN)$_2$]Br, as investigated by pump-probe spectroscopy. A reduction of U_{dimer} is optically induced by molecule displacement in the dimer under intradimer excitation. The mechanism of this metallization differs greatly from the photodoping-type mechanism reported previously. In contrast, a faster transition via the photodoping mechanism is detected for interdimer excitation. A metallic-domain-wall oscillation originating from the modulation of U_{dimer} was also observed near the critical end point of the Mott transition line.

DOI: 10.1103/PhysRevLett.103.066403 PACS numbers: 71.30.+h, 74.70.Kn, 78.30.Jw

The Mott insulator-metal transition is a central issue in a highly correlated electron system. In this transition, intersite transfer energy t competing with on-site Coulomb energy U can be controlled by modulating the correlation strength U/t. Mott insulator-metal-superconductivity transitions in transition metal oxides [1] and organic compounds [2,3] are induced by controlling electronic band filling (filling control, FC) and t (bandwidth control, BC). A κ type (BEDT-TTF)$_2X$ salt [where BEDT-TTF is bis (ethylenedithio)-tetrathiafulvalene and where X denotes a counter anion] [4] is a typical two-dimensional organic Mott insulator system. Figure 1 shows that the BEDT-TTF layer has a unit comprising a pair of BEDT-TTF molecules (BEDT-TTF dimer). If an effective on-site Coulomb energy U_{dimer} is larger than a critical value, which is usually of the order of the bandwidth and proportional to interdimer (or equivalently intersite) transfer energy t, then electrons are localized on each dimer site in a Hubbard model, forming a dimer Mott insulator. Various electronic properties have been observed using physical and chemical methods for tuning of bandwidth [5–10]. The BC phase diagram of κ type (BEDT-TTF)$_2X$ salt as shown in Fig. 1, comprising Mott insulator and metal (superconductor) phases separated by a characteristic curved boundary, is drawn by changing chemical pressure through deuteration of BEDT-TTF and substitutions of X, or by changing of external pressure.

Optical excitation is another technique for inducing an insulator-to-metal (I-M) transition [11,12]. Mechanisms of photoinduced I-M transitions (PIMTs) have been classified into FC type [13,14] or BC type [15], which are triggered by photocarrier doping (FC type) or nonlinear excitation of phonon modulating t (BC type). Further, a third type of PIMT—caused by optical modulation of U_{dimer}—is expected to be achieved in the dimer Mott insulator, having an intradimer degree of freedom. Because $U_{\mathrm{dimer}} = \frac{U}{2}[1 - \sqrt{1 + (4t_{\mathrm{dimer}}/U)^2}] + 2t_{\mathrm{dimer}} \cong 2t_{\mathrm{dimer}}$ for $U \gg t_{\mathrm{dimer}}$ [4], U_{dimer} is expected to be optically controlled by the modulation of t_{dimer}, where t_{dimer} is the intradimer transfer integral.

In this Letter, we report PIMT in an organic dimer Mott insulator under intradimer and interdimer excitations, as

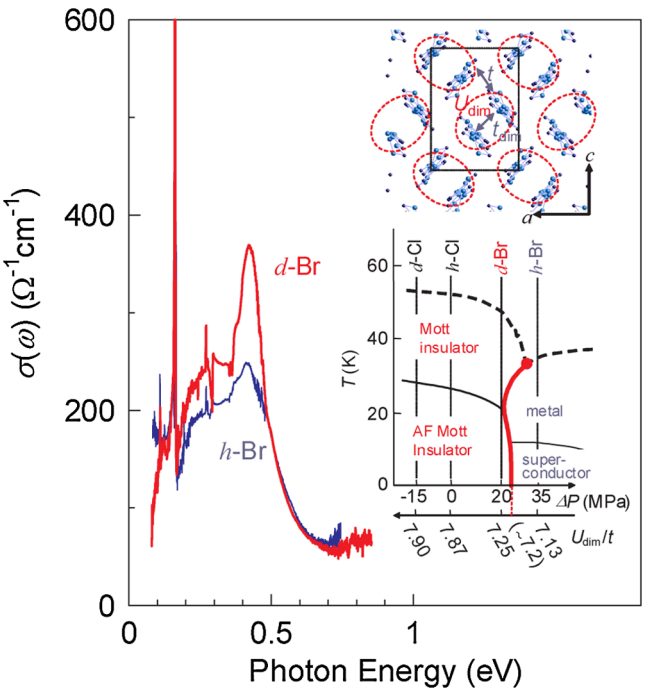

FIG. 1 (color online). Optical conductivity $\sigma(\omega)$ spectra of d-Br [light gray (red)] and h-Br [dark gray (blue)] at 10 K, together with the molecular arrangement of the BEDT-TTF layer (ac plane). The phase diagram of κ-(BEDT-TTF)$_2X$ as functions of external pressure and U_{dimer}/t is drawn by changing the deuteration of BEDT-TTF and substitutions of X. (AF denotes antiferromagnetic.)

investigated by femtosecond midinfrared spectroscopy. For intradimer excitation, the PIMT is driven by optical modulation of ~0.4%–0.7% of U_{dimer}, resulting from small intradimer molecular displacement. Furthermore, for interdimer excitation, an FC type PIMT mechanism is observed to occur.

We used the deuterated κ-(d-BEDT-TTF)$_2$Cu[N(CN)$_2$]Br (d-Br, where d represents the deuteration) and κ-(d-BEDT-TTF)$_2$Cu[N(CN)$_2$]Cl (d-Cl) which are positioned as insulators, respectively, near to and away from the first-order I-M phase boundary, although hydrogenated κ-(h-BEDT-TTF)$_2$Cu[N(CN)$_2$]Br (h-Br) is a metal (Fig. 1). Single crystals of d-Br, d-Cl, and h-Br (typical size: 1 × 1 × 0.5 mm) were prepared using a method described in the literature [5]. Then reflection-detected pump-probe measurements were performed using a Ti:Al_2O_3 amplifier system with custom-made optical parametric amplifiers. The pump and probe photon energies were 0.89, 0.63, and 0.32 eV (pump) and 0.1–0.7 eV (probe). The time resolution was 150 fs.

Optical conductivity $\sigma(\omega)$ spectra of the dimer Mott insulator d-Br and metallic h-Br are obtained by carrying out a Kramers-Kronig transformation of the reflectivity (R) spectra, as shown in Fig. 1. The peak at 0.45 eV and a lower energy shoulder are attributable to the intradimer (bonding to antibonding) transition and interdimer Hubbard gap transition, respectively [16]. Insets of Figs. 2(a) and 2(b) show the differential spectrum between h-Br and d-Br at 10 K [$\Delta R_{h\text{-}d}/R_d$; light gray (red) curve] and that for d-Br between 80 and 10 K [$\Delta R_{\mathrm{temp}}/R_{10}$; dark gray (blue) curve], which reflect the I-M transition and the temperature increase, respectively. The characteristic increase in $\Delta R_{h\text{-}d}/R_d$ around <0.4 eV [light gray (red) shade] is attributable to a Drude-like reflection, although the decrease in $\Delta R_{\mathrm{temp}}/R_{10}$ around 0.2–0.6 eV [dark gray (blue) shade] reflects the thermal excitation of carriers against the small activation energy.

Figures 2(a) and 2(b) show transient reflectivity ($\Delta R/R$) spectra of d-Br and d-Cl at time delays t_d of 0.1 and 2 ps, respectively, under excitation at 0.89 eV. Actually, intradimer bonding to antibonding transition mainly contributes to $\sigma(\omega)$ at 0.89 eV. For d-Br, immediately after photoirradiation, $\Delta R/R$ shows a negative value attributable to bleaching of the intradimer transition by the photocarrier generation. Then the amplitude of the Drude-like reflection at <0.4 eV increases. The $\Delta R/R$ spectrum at $t_d = 2$ ps is analogous to $\Delta R_{h\text{-}d}/R_d$, indicating the occurrence of PIMT. On the other hand, for d-Cl, $\Delta R/R$ decreases at <0.4 eV for any time delay, indicating that the PIMT does not occur at all. The efficiency of PIMT for d-Br was estimated as 50 dimers/photon from the fact that $\Delta R/R$ at 0.3 eV was approximately 10% of $\Delta R_{h\text{-}d}/R_d$; the photon density was 0.1 mJ/cm^2 (i.e., 1 photon/500 molecules).

Figure 3(a) shows time evolutions of the $\Delta R/R$ for d-Br observed at 0.26 eV, which indicate generation of the

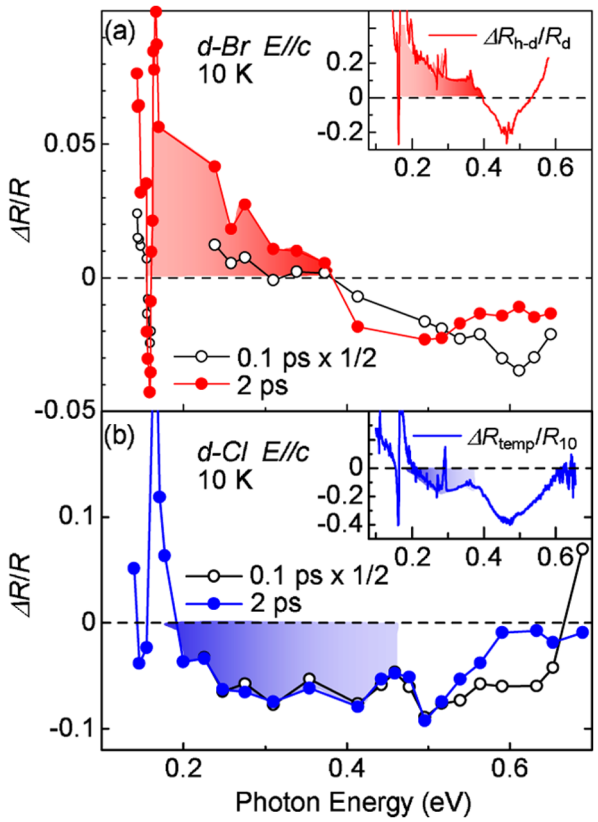

FIG. 2 (color online). (a, b) $\Delta R/R$ spectra at $t_d = 0.1$ ps and 2 ps for d-Br (a) and d-Cl (b) under excitation of 0.89 eV. Insets of (a) and (b) present differential spectra between h-Br and d-Br [(a) $\Delta R_{h\text{-}d}/R_d$; light gray (red) curve] at 10 K and between 80 and 10 K [(b) $\Delta R_{\mathrm{temp}}/R_{10}$; dark gray (blue) curve] of d-Br.

metallic state. The time profile, which reflects metallization, is reproduced by the equation $\frac{\Delta R(t)}{R} = -A\exp(-\frac{t}{\tau_g}) + B\exp(-\frac{t}{\tau_1})$ as shown by the solid green curve, where $A = -1.44$, $\tau_g = 1.1$ ps, $B = 2.44$, and $\tau_1 = 70$ ps. It is noteworthy that the generation time of the metallic state τ_g is considerably longer than the time scale (ca. 40 fs) of the intersite charge transfer, suggesting that the I-M transition occurs because of the intermolecular motion and not the photocarrier doping [17,18].

The oscillating structure in the time evolution of $\Delta R/R$ at 0.26 eV also shows the contribution of the intermolecular coherent motion to the PIMT. The time profile and Fourier transformed spectrum of the oscillating component $\Delta R_{\mathrm{osc}}(t)/R$ for d-Br are shown in Figs. 3(b) and 3(d), respectively. Analyses were carried out using the equation $\Delta R_{\mathrm{osc}}(t) = \sum_{i=1}^{4} A_i[1-\exp(-t/\tau_{ri})]\exp(-t/\tau_i)\cos(\omega_i t - \phi_i)$, and the oscillating frequencies $\omega_i (i = 1\text{–}4)$ were estimated to be 16, 27, 45, and 59 cm^{-1}. Here, τ_{ri}, τ_i, and ϕ_i represent the rise and decay time constant and the initial phase for each oscillation, respectively. Actually, ϕ_i is smaller than 0.1π, indicating a cosinelike oscillation, which is detected in the photoinduced phase transition, and is attributable to

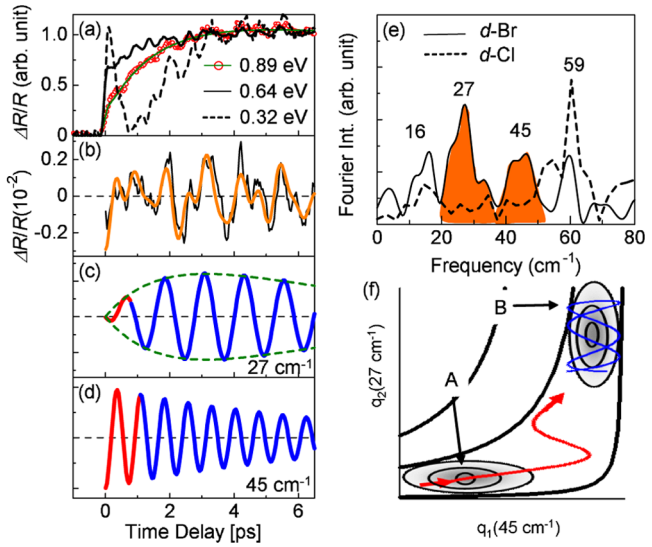

FIG. 3 (color online). (a) Time evolutions of $\Delta R/R$ for d-Br detected at 0.26 eV under excitation at 0.89 eV (red circles with green fitted curve), 0.64 eV (solid curve), and 0.32 eV (dashed curve). (b) Time profile of the oscillating component of $\Delta R/R$ for d-Br (0.89 eV excitation). (c, d) The 27 cm^{-1} (b) and 45 cm^{-1} (c) cosinelike oscillations, which were obtained through analysis (see the text). (e) Fourier transformed spectra of the oscillation for d-Br and d-Cl. (f) Classical trajectories representing coherent phonon dynamics in the potential surface. A and B, respectively, denote the excited Mott insulator state and the photoinduced metallic state.

the displacive excitation of the coherent phonon in the photoexcited state or the photoinduced metallic state [14,17,18], and not in the ground state. Among these oscillations, the 27 cm^{-1} and 45 cm^{-1} modes are not detected in d-Cl, as shown by the dashed curve in Fig. 3(e). Accordingly, these two modes are related to the PIMT. It is noteworthy that the 27 cm^{-1} mode shows a finite rise time of $\tau_{r2} = 1$ ps [Fig. 3(c)], which is identical to the time scale of metallization t_g, whereas the 45 cm^{-1} mode appears instantaneously [Fig. 3(d)]. Therefore, as shown by the classical trajectories in the q_1(45 cm^{-1})–q_2(27 cm^{-1}) potential surface [Fig. 3(f)], the 45 cm^{-1} mode phonon is considered to be induced along the q_1 axes [light gray (red) curve] immediately after generation in the photoexcited insulator state (A); then the 27 cm^{-1} mode oscillates along the q_2 axis [dark gray (blue) curve] in the metallic state (B). Observation of the 27 cm^{-1} mode in the Raman spectrum of metallic h-Br [19] supports the above mentioned consideration. Possible candidates for such coherent low-frequency phonons are intradimer molecular motions, which effectively modulate the t_{dimer}, i.e., the intradimer molecular displacements such as stretching and libration, which are triggered by the bonding to the antibonding excitation, causing a decrease in t_{dimer} and $U_{\mathrm{dimer}}/2$; this results in metallization.

To confirm such U_{dimer} modulation in the PIMT mechanism, we also investigated the PIMT dynamics under interdimer Hubbard gap excitation. The black solid and dashed curves in Fig. 3(a) denote time evolutions of $\Delta R(t)/R$ under excitation at 0.64 eV and 0.32 eV, respectively. In these energy regions, contributions from both intradimer and interdimer transitions are substantial, although the interdimer component becomes dominant at lower energies. Even at these excitation energies, increases in reflectivity at 0.26 eV are detected, confirming the occurrence of the PIMT. However, the buildup time of the PIMT differs from the result of the 0.89 eV excitation; i.e., the immediate (< 0.2 ps) response is detected for 0.64 and 0.32 eV excitations. Such ultrafast responses are attributed to the photocarrier doping or, equivalently, the FC type mechanism. Moreover, for the 0.32 eV excitation, a fast decay of 0.4 ps is observed. Such rapid decay is attributable to the ultrafast relaxation of the metallic state, which has been reported in other FC type PIMTs [12–14]. Therefore, the optical modulation of U_{dimer} through the intradimer molecular displacement is confirmed to be induced solely in the case of the intradimer excitation, although the ultrafast FC type PIMT occurs for interdimer excitation.

Next, we roughly evaluate the photoinduced intradimer molecular displacement and corresponding change in U_{dimer} ($\Delta U_{\mathrm{dimer}}$) more quantitatively. Here, U_{dimer} and t of pristine samples are calculated as $U_{\mathrm{dimer}} \cong 2t_{\mathrm{dimer}}$, $t \cong |t_p + t_q|/2$, where t_p and t_q are anisotropic interdimer transfer integrals calculated using the extended Huckel method with structural data [20]. In the past, U_{dimer}/t for the phase boundary was also estimated from precise studies of the phase diagram of κ-[(h-BEDT-TTF)$_{1-x}$ × (d-BEDT-TTF)$_x$]$_2$Cu[N(CN)$_2$]Br [21]. Considering that U_{dimer}/t values for d-Br and the I-M boundary are calculated as 7.25 and 7.2–7.22, respectively, as shown in Fig. 1, observation of PIMT reveals that the change of U_{dimer}/t upon PIMT is approximately 0.4%–0.7%. Therefore, U_{dimer} is estimated as ~0.4%–0.7% because the photoinduced change in U_{dimer}/t is mainly attributable to the $\Delta U_{\mathrm{dimer}}$. Such a small change of U_{dimer} is indicative of small molecular displacements. If we simply assume that the intradimer relative molecular distances are changed for reducing t_{dimer} to $\sim U_{\mathrm{dimer}}/2$, the magnitude of the displacement is as small as 0.05% of the molecular distance in the dimer. Further, U_{dimer}/t for d-Cl is 7.87; therefore, $\Delta U_{\mathrm{dimer}}$ must be greater than 9% for inducing the PIMT. A very large displacement of 0.5% is necessary for obtaining such a large $\Delta U_{\mathrm{dimer}}$ value, which might be the reason why the PIMT is not detected in d-Cl.

Next, we discuss the slower dynamics occurring after the PIMT is completed. The photoinduced I-M domain wall (DW), which is a highly nonequilibrium state, is expected to exhibit novel properties near the critical end point of the first-order phase boundary in Fig. 1 [5,6]. The inset of Fig. 4(a) shows time evolutions of $\Delta R/R$ at 0.31 eV, indicating generation of the metallic state. The most impressive feature of the time evolution is the oscillating structure

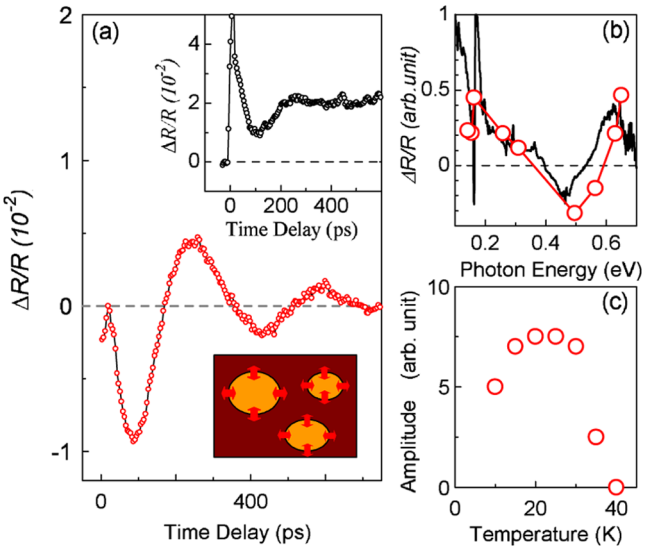

FIG. 4 (color online). (a) Time evolutions of $\Delta R/R$ (inset) and the oscillating component detected at 0.31 eV for the slow time domain, together with a schematic illustration of the oscillating photoinduced metallic domain. (b) Amplitude spectrum of the photoinduced metallic state is shown by the red circles. The solid curve represents $\Delta R_{h\text{-}d}/R_d$. (c) Oscillating amplitude as a function of temperature.

with a period of 340 ps, which is estimated from the oscillating component shown by light gray (red) circles. The frequency of oscillation is independent of the probe energy. The amplitude spectrum shown by the red circles portrayed in Fig. 4(b) is analogous to the $\Delta R_{h\text{-}d}/R_d$ (solid curve in Fig. 4(b)]. Accordingly, such a long-period oscillation is attributable not to propagating or standing acoustic waves [22] but to the coherent modulation of the metallic volume fraction, suggesting the oscillating DW motion. Such interpretation using the DW picture is supported by the real-imaging observation of the phase separation near the phase boundary in the BC Mott transition [23]. The DW oscillation of such a kind is considered to be driven by the thermodynamic instability of the photoinduced state. Usually, it is disturbed by the I-M energy difference, potential barrier, and dephasing process occurring via an electron-lattice interaction. However, for the PIMT in *d*-Br, the I-M energy difference and the barrier height between phases are tuned to be very small near the characteristic curved phase boundary and the critical end point at 35–40 K because the molecular displacement with the I-M transition is very small. In fact, the oscillating amplitude shows a maximum at approximately 25 K, as shown in Fig. 4(c).

In summary, our results demonstrate the optical modulation of U_{dimer} and the resultant PIMT in the dimer Mott insulator κ-(*d*-BEDT-TTF)$_2$Cu[N(CN)$_2$]Br. Under intradimer excitation, the PIMT is driven by the intradimer molecular displacements, which decrease U_{dimer} by approximately 0.4%–0.7%. Such a small molecular displacement with the PIMT enables the detection of an oscillating DW motion. Furthermore, an FC type ultrafast PIMT is detected under interdimer Hubbard gap excitation.

We would like to thank T. Mori for valuable discussions. This study was supported by Grants-in-Aid for Scientific Research (Innovative Areas "New Frontier in Materials Science Opened by Molecular Degrees of Freedom," No. 20110005, and B, No. 20340069, No. 20340095).

*s-iwai@m.tains.tohoku.ac.jp

[1] M. Imada, A. Fujimori, and Y. Tokura, Rev. Mod. Phys. **70**, 1039 (1998).
[2] Molecular Conductors, edited by P. Batail [Chem. Rev. **104**, 4887 (2004)].
[3] R. H. McKenzie, Science **278**, 820 (1997).
[4] K. Kanoda, Hyperfine Interact. **104**, 235 (1997).
[5] F. Kagawa, K. Miyagawa, and K. Kanoda, Nature (London) **436**, 534 (2005).
[6] M. de Souza *et al.*, Phys. Rev. Lett. **99**, 037003 (2007).
[7] T. Sasaki *et al.*, Phys. Rev. B **69**, 064508 (2004).
[8] D. Faltermeier *et al.*, Phys. Rev. B **76**, 165113 (2007).
[9] M. Dumm *et al.*, Phys. Rev. B **79**, 195106 (2009).
[10] T. Sasaki *et al.*, Phys. Rev. Lett. **101**, 206403 (2008).
[11] *Photoinduced Phase Transition*, edited by K. Nasu (World Scientific, Singapore, 2004).
[12] Special Topic on Photo-Induced Phase Transition and Their Dynamics, edited by M. Gonokami and S. Koshihara [J. Phys. Soc. Jpn. **75**, 011 001 (2006)].
[13] S. Iwai *et al.*, Phys. Rev. Lett. **91**, 057401 (2003).
[14] L. Perfetti *et al.*, Phys. Rev. Lett. **97**, 067402 (2006).
[15] M. Rini *et al.*, Nature (London) **449**, 72 (2007).
[16] M. J. Rozenberg *et al.*, Phys. Rev. Lett. **75**, 105 (1995).
[17] M. Chollet *et al.*, Science **307**, 86 (2005).
[18] S. Iwai *et al.*, Phys. Rev. Lett. **98**, 097402 (2007).
[19] T. Sekine *et al.*, Synth. Met. **70**, 981 (1995).
[20] M. Watanabe, doctoral thesis, Okayama University, 1999.
[21] N. Yoneyama, T. Sasaki, and K. Kobayashi, J. Phys. Soc. Jpn. **73**, 1434 (2004).
[22] A. M. Lindenberg *et al.*, Phys. Rev. Lett. **84**, 111 (2000).
[23] T. Sasaki *et al.*, Phys. Rev. Lett. **92**, 227001 (2004).